Evidence for the Presence of a Guanine Quadruplex Forming Region within a Polypurine Tract of the Hypoxia Inducible Factor 1α Promoter[†]

Richard De Armond, Stacey Wood, Daekyu Sun, Laurence H. Hurley, and Scot W. Ebbinghaus*

Arizona Cancer Center, University of Arizona, 1515 North Campbell Avenue, Tucson, Arizona 85724-5024

Received August 13, 2005; Revised Manuscript Received October 2, 2005

ABSTRACT: The promoter of the hypoxia inducible factor 1 alpha (HIF-1α) gene has a polypurine/polypyrimidine tract (−65 to −85) overlapping or adjacent to several putative transcription factor binding sites, and we found that mutagenesis of this region diminished basal HIF-1α expression. Oligonucleotides representing this region of the HIF-1α promoter were analyzed by electrophoretic mobility shift, chemical probing, circular dichroism, and DNA polymerase arrest assays. The guanine-rich strand was found to form a parallel, unimolecular quadruplex in the presence of potassium that was further stabilized by two known quadruplex binding compounds, the cationic porphyrin TmPyP4 and the natural product telomestatin, while TmPyP2, a positional isomer of TmPyP4, did not stabilize quadruplex formation. These data suggest that a quadruplex structure may form in a region of the HIF-1α promoter that regulates basal HIF-1α expression.

Hypoxia inducible factor 1 (HIF-1)[1] is a transcription factor composed of a hypoxia inducible alpha subunit (HIF-1α) and a constitutively expressed beta subunit (HIF-1β) responsible for the regulation of over 60 genes involved in oxygen homeostasis (*1*, *2*). HIF-1α is overexpressed in many common human tumors as a result of intratumoral hypoxia (*3*). HIF-1α levels are normally undetectable in normoxia due to posttranslational processing involving proline hydroxylation and the von Hippel Lindau (VHL) protein, a multifunctional adapter molecule that mediates the ubiquitinylation of HIF-1α, targeting it to the proteasome for degradation (*2*). During hypoxia, HIF-1α accumulates, translocates to the nucleus, and dimerizes with HIF-1β. The HIF-1 heterodimer then binds to a DNA consensus sequence known as the hypoxia response element (HRE) (*4*). In tumors, the activation of hypoxia responsive genes leads to angiogenesis, metabolic adaptation, resistance to apoptosis, and the expression of a variety of genes associated with local invasion or metastasis (*5*, *6*). The vascular endothelial growth factor (VEGF) gene is an example of a gene activated by HIF-1. VEGF is a pro-angiogenic ligand secreted by many tumors that binds to tyrosine kinase receptors (VEGF-R1 and -R2) expressed predominantly on angioblasts and endothelial cells, recruiting these cells to form neovessels in the tumor (*7*).

HIF-1α may be abnormally overexpressed in the absence of hypoxia by several mechanisms, such as the loss of the VHL tumor suppressor gene, a frequent event in renal cell carcinoma that disrupts the usual posttranslational regulation of HIF-1α in normoxia (*8*). HIF-1α levels may also be controlled under normoxia by the rate of HIF-1α translation in certain types of cells in response to hormones, growth factors, or cytokines. This alternate pathway of HIF-1α regulation appears to involve signaling through the phosphatidyl inositol 3 kinase (PI3K) pathway, resulting in the activation of the p70S6K translation factor through mTOR (molecular target of rapamycin) and involves the recognition of a 5′-terminal oligopyrimidine tract (5′-TOP) in the HIF-1α mRNA (*9*−*15*).

In most cells, HIF-1α mRNA levels do not increase in hypoxia compared to normoxia, but elevated levels of HIF-1α mRNA can be detected in some human tumor specimens or induced by hypoxia in certain mammalian cells (*12*, *16*−*21*). Transcriptional upregulation of HIF-1α gene expression is another mechanism of inducing HIF-1α expression by nonhypoxic stimuli in certain cell types, such as angiotensin II in vascular smooth muscle cells (*12*) and lipopolysaccharide in macrophages (*22*). Transcriptional upregulation of HIF-1α expression by angiotensin II was shown to require the presence of the untranslated region (5′UTR) of the HIF-1α gene and involve signaling through the protein kinase C (PKC) pathway (*12*). Human and murine HIF-1α promoters are highly conserved (*23*), and HIF-1α transcription is predominantly controlled by a 200 base pair (bp) core promoter upstream of the transcription start site and the 287 bp 5′UTR (*24*). Functional elements of the HIF-1α promoter were identified by transient expression of reporter gene constructs containing serial 5′ deletions in normoxic and cobalt chloride treated endothelial and tumor cell lines (*24*).

[†] Funding for this work was provided by grants from the U. S. Army Medical Research and Materiel Command (W81WXH-04-1-0560), National Insitutes of Health (CA85306 and CA19466) and the Flinn Foundation (1580).

* To whom correspondence should be addressed. Phone: 520-626-3424. Fax: 520-626-5462. E-mail: sebbinghaus@azcc.arizona.edu.

[1] Abbreviations: HIF-1α, hypoxia inducible factor 1 alpha; VHL, Von Hippel Lindau; HRE, hypoxia response element; VEGF, vascular endothelial growth factor; PI3K, phosphatidyl inositol 3 kinase; mTOR (molecular target of rapamycin; 5′ TOP, 5′ terminal oligopyrimidine tract); 5′UTR, 5′ untranslated region; PKC, protein kinase C; G-quadruplex, guanine quadruplex; PPT, polypurine tract; TmPyP2, 5,-10,15,20-tetra(*N*-methyl-2-pyridyl)porphin; TMPyP4, 5,10,15,20-tetra-(*N*-methyl-4-pyridyl)porphin; ODNs, oligodeoxyribonucleotides; DMS, dimethyl sulfate; CD, circular dichroism.

10.1021/bi051618u CCC: $30.25
Published on Web 11/12/2005

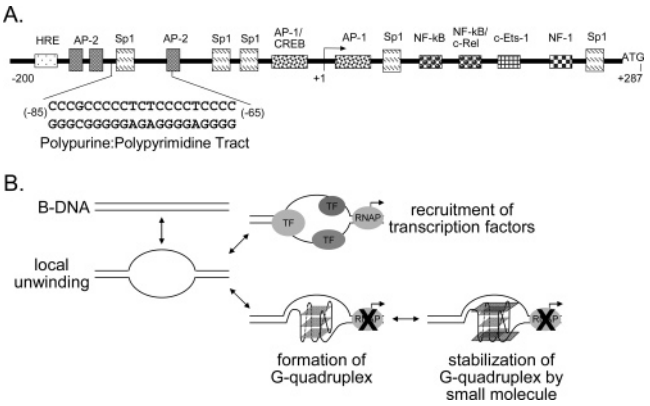

FIGURE 1: (A) Schematic representation of the minimal HIF-1α promoter highlighting putative transcription factor binding site assignments and the polypurine/polypyrimidine tract. (B) Model of promoter silencing by guanine quadruplex formation.

The human HIF-1α promoter lacks a TATA box, but contains putative binding sites for Sp1, NF-1, AP-1, AP-2, and HIF-1 upstream of the transcription initiation site as well as several putative transcription factor binding sites in the 5′UTR (*23*, *24*).

The critical cis-acting elements involved in the transcriptional upregulation of HIF-1α in hypoxia are located in the first 100 bp of the HIF-1α promoter (*24*). Within this region, there is a mostly uninterrupted polypurine:polypyrimidine tract from −85 to −65 upstream of the transcription start site and overlapping putative Sp1 and Ap-2 binding sites (Figure 1). Guanine-rich sequences can associate into four-stranded structures formed from stacks of guanine tetrads, and sequences conforming to a motif potentially capable of forming such structures have been reported to be relatively common in the human genome (*25*−*29*). The Hoogsteen-bonding of the guanine tetrads is favored by the presence of a monovalent cation, especially potassium, which fits within a central core formed by the carbonyl groups of the guanines (*30*, *31*). Intermolecular guanine quadruplexes can form from the association of two or four strands of DNA (or RNA), and such structures may form under physiological conditions by the human immunodeficiency virus RNA and by some guanine-rich aptameric oligonucleotides (*32*−*39*). Intramolecular guanine quadruplexes form by the folding of a single strand, and guanine-rich sequences that are potentially capable of forming these structures can be found in telomeric DNA from humans, most eukaryotes, and several lower organisms (*40*−*49*). Sequences derived from the human immunoglobin switch region, insulin gene, and fragile X syndrome gene are also capable of forming quadruplexes (*50*−*53*). The DNA helicases that are deficient in Bloom's syndrome and Werner's syndrome can recognize quadruplex DNA, suggesting that these structures form in cells and if not resolved lead to difficulties during DNA recombination (reviewed in ref *54*). Recently, guanine-rich sequences from a nuclease hypersensitivity element of the human c-myc oncogene promoter were shown to form several different quadruplex structures and appear to be important in regulating c-myc transcription (*55*−*58*). Additional evidence for G-quadruplexes in the regulatory regions of human genes was reported for three muscle-specific genes (*59*). The human telomeric G-quadruplex has been studied as a target for drug development for the treatment of cancer, and several DNA binding compounds have a preference for quadruplex DNA (*60*−*62*). Silencing gene expression by ligand interaction with a G-quadruplex in a gene promoter is illustrated in Figure 1 and has been described for the c-myc oncogene. Molecules capable of binding to the G-quadruplexes formed by the c-myc promoter include TmPyP4, a cationic porphyrin; 307A, a 2,6-pyridin-dicarboxamide derivative; Hoechst 33258; and telomestatin, a natural product isolated from *Streptomyces anulatus* and previously shown to be a potent telomerase inhibitor (*58*, *63*−*66*).

In the present work, we wished to investigate the importance of the polypurine tract (PPT) in the HIF-1α promoter to HIF-1α transcription and determine whether the guanine-rich strand of this element could form an intramolecular quadruplex. Substitution mutations in the PPT markedly diminished basal HIF-1α expression in Caki-1 (VHL wild-type kidney cancer) cells. Dimethyl sulfate footprinting and circular dichroism studies of oligonucleotides representing the guanine-rich strand of the HIF-1α PPT suggest the formation of a unimolecular quadruplex in the presence of potassium, and DNA polymerase arrest assays show stabilization of the quadruplex with TmPyP4 and telomestatin. The solution structure for the c-myc quadruplex has been recently reported (*67*, *68*), and based on the presence of similar $G_3NG_3N_6G_3NG_3$ sequence motifs in the quadruplex forming regions of both the HIF-1α promoter and the more thoroughly studied c-myc promoter, we suggest that a similar structure forms in the HIF-1α promoter and may play a role in regulating HIF-1α gene expression.

MATERIALS AND METHODS

Chemical Reagents and Oligonucleotides. 5,10,15,20-Tetra(*N*-methyl-2-pyridyl)porphin (TMPyP2) and 5,10,15,-20-tetra(*N*-methyl-4-pyridyl)porphin (TMPyP4) were purchased from Mid-Century Chemicals (Posen, IL). Telomestatin was a gift from Dr. Kazuo Shin-ya (University of Tokyo, Japan). Oligodeoxyribonucleotides (ODNs) were purchased from commercial vendors and gel purified. Concentrations were determined by absorbance measurements at 260 nm using the weighted sum method to calculate the molar extinction coefficient for each ODN according to its composition (*69*). Calculated extinction coefficients for the ODNs are presented as Supporting Information. The sequences of the ODNs used in these studies are given in Table 1 and shown schematically in Figure 3.

Electrophoretic Mobility Shift Assays. PAGE-purified oligonucleotides were end-labeled by the T4 polynucleotide kinase reaction, purified on spin columns, and eluted into pure water. In the experiment illustrated in Figure 5A, G-quadruplex formation was performed by diluting the ODNs to a final concentration of 0.1 μM in a buffer containing 50 mM Tris-Cl (pH 7.6) with or without 140 mM KCl, heating the solution to 95 °C for 5 min and then slow cooling to room temperature over 3−4 h. The solutions were weighted by adding 50% glycerol (v/v, without dyes) to a final concentration of 5% and loaded onto a 12% nondenaturing, high-potassium polyacrylamide gel containing 90 mM Tris-Cl, 90 mM borate, 1 mM EDTA, and 140 mM KCl (pH 8.0). The electrophoresis was performed at room temperature at 10 V/cm for 6 h, and the electrophoresis running buffer contained 90 mM Tris-Cl, 90 mM borate, 1 mM EDTA (1× TBE) without KCl. In the experiment

Table 1: Oligonucleotide Sequences[a] and Summary of DMS Footprinting and CD Spectroscopy

ODN	Sequence (5′→3′)	DMS Footprint	CD 260 nm peak
I	CGCGCTCCCGCCCCCTCTCCCCTCCCCGCGC	no	no
II	GCGCGGGGAGGGGAGAGGGGGCGGGAGCGCG	yes	yes
III	GGGGAGGGGAGAGGGGGCGGGA	yes	yes
IV	**TCGGGC-** GCGCGGGGAGGGGAGAGGGGGCGGGAGCGCG	yes	no
V	**CAGGGGGCGGGCAAGGGCGGAGGCGCGCTCGGGC**	no	ND
VI	**CAGGGGGCGGGCAAGGGCGGAGGCGCGCTCGGGC-** GCGCGGGGAGGGGAGAGGGGGCGGGAGCGCG	yes	ND
VII	GCGCGGGGAGGGGAGAGGGGGCGGG**ga**CGCG	yes	yes
VIII	GCGCGG**c**GAG**c**GGAGAGGG**c**GCG**c**GAGCGCG	no	no
IX	GCGCGGGGAGGG**ctctcc**GGGCGGGAGCGCG	no	no
X	GCGCGGGGAGGGG**tct**GGGGGCGGGAGCGCG	yes	yes
XI	GCGCGGGGAGGG**ctct**GGGGGCGGGAGCGCG	weak	no
XII	GCGCGGGGAGGGG**tctc**GGGGCGGGAGCGCG	yes	yes
XIII	GCGCGGGGAGGGG**tctcc**GGGCGGGAGCGCG	weak	no
XIV	GCGCGGGGAGGG**ctctc**GGGGCGGGAGCGCG	weak	no
myc1245	**t**GGGGAGGG**ttttta**GGG**t**GGG**ga**	yes	ND
polP	TAATACGACTCACTATAGCAATTGC		
polH	TCCAACTATGTATACGCGCGGGGAGGGGAGAGGGGCGGGAGCGCGTTAGCGACACGCAATT*GCTATAGTGAGTCGTATTA*		
polC	TCCAACTATGTATACTACGTATTCAGCTCATGCTATACGTCATCGTTAGCGACACGCAATT*GCTATAGTGAGTCGTATTA*		

[a] Polypurine sequences are aligned with ODN II where applicable. Bold uppercase sequence represents the sequence adjacent to ODN II in the HIF-1α promoter. Bold lowercase nucleotides represent substitutions in ODN II. The DNA polymerase arrest templates contain the sequence of ODN II (underlined in polH) or a random control sequence (underlined in polC) upstream of the polP primer binding site (italics). ND, not done.

illustrated in Figure 5B, G-quadruplex formation was performed by diluting ODN II to a final concentration of 0.1 μM in a buffer containing 10 mM Tris-Cl (pH 7.4) plus either 140 mM KCl, 140 mM NaCl, or no additional salt. The solutions were heated to 95 °C for 5 min, slowly cooled to 37 °C over 2−3 h, and then DMS was added to a final concentration of 0.25%. The solutions were weighted with glycerol, and immediately loaded onto a 10% nondenaturing, low-potasium polyacrylamide gel buffered with 1× TBE plus 10 mM KCl, resulting in a total DMS incubation time of under 5 min. Electrophoresis was performed at room temperature at 10 V/cm for 6 h followed by autoradiography. A separate set of samples was handled identically except that DMS was not added, demonstrating that the DMS treatment did not alter the electrophoretic mobility of ODN II (not shown). The bands indicated in Figure 5B were excised from the gel, and the DMS treated ODN was eluted in gel elution buffer (500 mM ammonium acetate, 10 mM magnesium acetate, and 1 mM EDTA, pH 8.0) at 37 °C for 4 h. The gel eluate containing the DMS treated ODN was concentrated and washed using Sep-Pak C18 columns, eluted from the columns in 60% methanol and lyophilized. The DMS treated ODNs were then dissolved in 10% piperidine for piperidine cleavage as described for DMS footprinting.

DMS Footprinting. The dimethyl sulfate (DMS) footprints for G-quadruplexes were performed using end-labeled ODNs according to the chemical sequencing method of Maxam−Gilbert essentially as described (*63*). G-quadruplex formation was performed as described above in 50 mM Tris-HCl (pH 7.6) with or without 140 mM KCl by heating the ODNs to 95 °C and slowly cooling to reoom temperature over 3−4 h. The solutions were treated with 0.25% DMS for 5 min. DMS stop solution [1.5 M sodium acetate (pH 7.0), 1 M β-mercaptoethanol, 250 μg/mL tRNA] was added, the ODNs were precipitated, treated with 10% (v/v) piperidine, evaporated to dryness, redissolved in formamide loading buffer, and loaded onto a 12% polyacrylamide sequencing gel.

DNA Polymerase Arrest Assay. The DNA polymerase arrest assay was performed by modification of previously reported methods (*70*, *71*). A 25-mer taq polymerase primer (polP) was end-labeled, and a 2-fold excess of primer was annealed to 0.5 pmol of taq polymerase template (polH or polC). The resulting asymmetric primer-template duplex was gel purified and eluted in 2× taq polymerase arrest assay buffer [120 mM Tris-HCl (pH 8.5), 30 mM ammonium sulfate, 15 mM $MgCl_2$]. The arrest assay was performed in a buffer of 60 mM Tris-HCl (pH 8.3), 15 mM ammonium sulfate, 7.5 mM $MgCl_2$, 1.5 mM dNTPs, 0 to 140 mM KCl, in a final volume of 10 μL. Primer-template duplex in the arrest assay buffer was incubated at 37 °C with 0−1 μM of TmPyP4, TmPyP2, or telomestatin. Reaction mixtures were brought to 47 °C, primer extension was initiated by adding 5 U of taq DNA polymerase (Fermentas, Hanover, MD), and the reaction was incubated at 47 °C for 20 min. Primer extension was stopped with 10 μL taq polymerase stopping buffer (95% formamide, 10 mM EDTA, 10 mM NaOH, 0.1% xylene cylanol, 0.1% bromophenol blue), denatured at 95 °C for 5 min, quickly cooled on ice, and primer extension products were separated on 10% sequencing gels. The arrest sites were identified by alignment with a chain termination

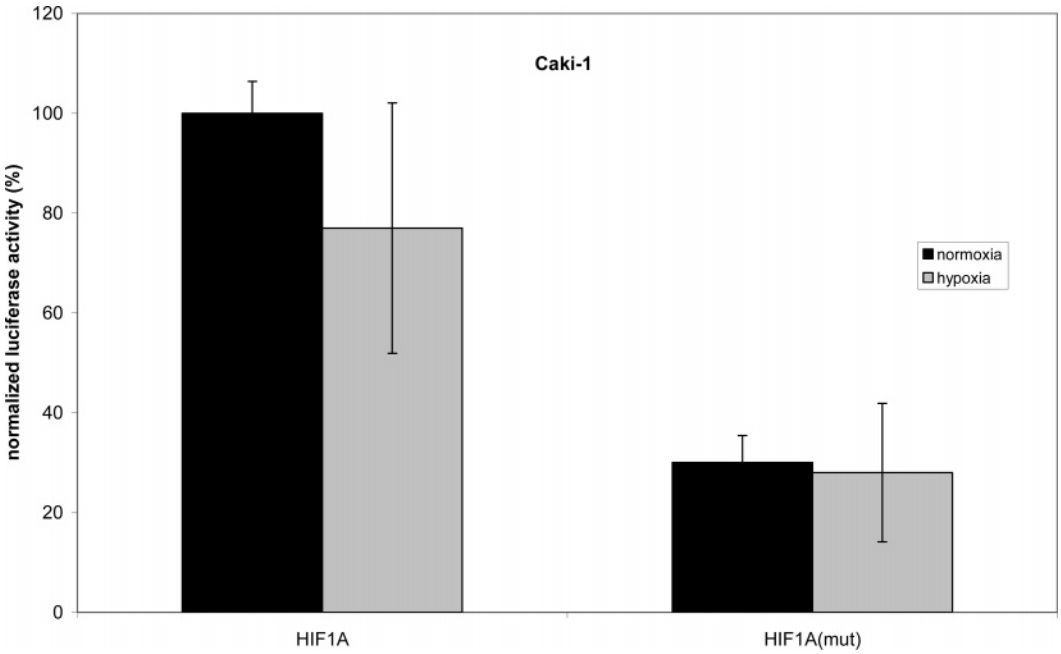

FIGURE 2: Transient transfection analysis shows that disruption of the PPT by substitution mutations diminishes HIF-1α expression in normoxia and hypoxia. Transfections were performed in duplicate, and the data represent the mean (± standard deviation) of normalized luciferase activity from three independent experiments.

sequencing reaction using the same primer−template duplex with the Thermosequenase kit (USB Corporation, Cleveland, OH) according to the manufacturer's instructions.

Circular Dichroism Spectroscopy. Circular dichroism (CD) spectra were measured on ODNs at a concentration of 100 μM in either 50 mM Tris-HCl, 25 mM NaCl, or 25 mM KCl. Spectra were measured on a Jasco-810 spectropolarimeter (Jasco, Easton, MD) using a quartz cell of 1-mm optical path length, an instrument scanning speed of 100 nm/min, with a response of 1 s, over a range of 200 to 350 nm. A set of three scans was averaged for each sample at 25 °C.

Transient Transfections. The plasmid pGL3/HIF1A was constructed as follows. The HIF-1α promoter from −538 to +291 (relative to the transcription start site) was amplified by polymerase chain reaction (PCR) from pooled human genomic DNA (Boehringer-Mannheim) using primers (forward: GAACAGAGAGCCCAGCAGAGTTGGGCGG and reverse: CCTCCATGGTGAATCGGTCCCCGCGATG) that were previously described (*24*). The amplicon was cloned into the pCR2.1-TOPO vector (Invitrogen), excised, ligated upstream of the luciferase gene in the pGL3 Basic vector (Promega), and the sequence of the insert of the resulting pGL3/HIF1A construct was confirmed. The PPT was disrupted in the plasmid pGL3/HIF1A^{mut} by multiple (fifteen) substitution mutations from −84 to −68 introduced by site-directed mutagenesis (top strand: CCGCCCCCTCTCCCCTC → GAATTCCTCGAGGAGCT; site-directed mutagenesis and sequencing were performed by Topgene, Canada). Caki-1 (VHL+/+ kidney cancer) cells were purchased from the American Type Culture Collection (ATCC, Manassas, VA) and grown under standard conditions. The transfection mixture for Caki-1 cells included 2 μg of pGL3/HIF1A or pGL3/HIF1A^{mut}, 20 ng pRL/SV40 (Promega), and 4 μL LT-1 (Mirus, Madison, WI). Cells at 70% confluence were transfected in RPMI for 2 h at 37 °C in normoxia, and then cells were incubated in either normoxia or hypoxia (1% O_2) at 37 °C for 24 h. Dual luciferase assays were performed with commercial reagents (Biotium, Hayward, CA) according to the manufacturer's instructions. The ratio of firefly to renilla luciferase activity was calculated, and normalized for the average firefly/renilla luciferase activity for pGL3/HIF1A in normoxia for each experiment. Transfections were performed in duplicate and repeated three times. The data presented in Figure 2 represent the mean (± standard deviation) normalized luciferase activity.

RESULTS

To determine whether the HIF-1α PPT was needed for basal HIF-1α transcription, we performed transient transfections on wild-type and PPT mutant HIF-1α promoters in Caki-1 cells. As shown in Figure 2, HIF-1α transcription is not induced by hypoxia in Caki-1 cells. The PPT was disrupted in pGL3/HIF1A^{mut} by introducing 15 substitution mutations between −84 to −68. Disrupting the PPT caused a 70% decline in HIF-1α expression both in normoxia and hypoxia in Caki-1 cells (Figure 2).

To determine whether the HIF-1α PPT could undergo a conformational shift to a DNA secondary structure, we evaluated the series of oligonucleotides (ODNs) illustrated in Figure 3 which represent native or mutant sequences from the HIF-1α promoter. These ODNs were used in footprinting, electrophoretic mobility shift, and circular dichroism studies in solution.

Hoogsteen hydrogen bonds render the N-7 position of guanines in a tetrad inaccessible to dimethyl sulfate (DMS), and the guanines involved in G-quadruplex formation can be detected by DMS footprinting. In Figure 4, the DMS cleavage patterns of ODNs I, II, III, and VIII are shown in the presence and absence of 140 mM potassium ions and compared to a homologous sequence derived from the c-myc promoter, myc1245, for which the solution structure determined by NMR has been reported (*67*). In the presence of potassium, strong footprints are produced by ODN II, ODN

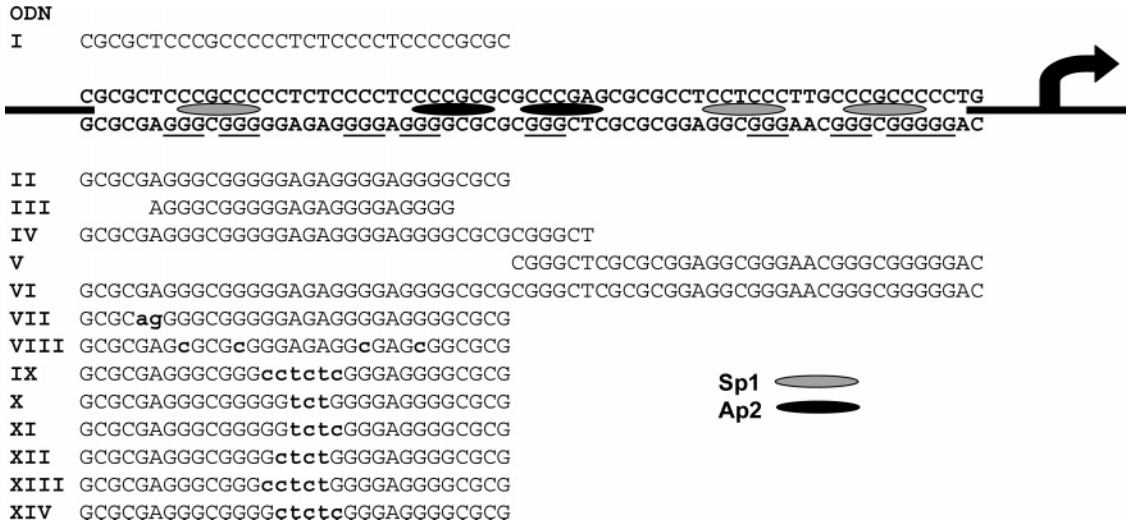

FIGURE 3: Oligonucleotides representing the HIF-1α promoter which were used to evaluate DNA secondary structure formation. ODN I is written in 5′ → 3′ orientation. ODNs II−XIV are written in 3′ → 5′ orientation and aligned with the bottom strand of the HIF-1α promoter. Mutated nucleotides are in lower case and bold. Runs of three or more guanines are underlined.

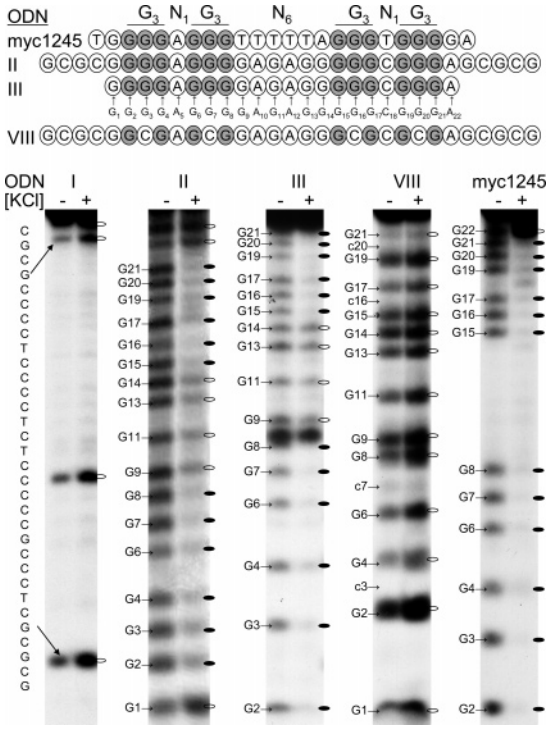

FIGURE 4: The sequences of oligonucleotides representing the quadruplex forming regions of the c-myc and HIF-1α promoters and conforming to the $G_3N_1G_3N_6G_3N_1G_3$ sequence motif are illustrated schematically. DMS footprinting reactions with ODNs representing the HIF-1α promoter in the absence (−) or presence (+) of 140 mM KCl in comparison with the footprint produced by the myc1245 ODN. In the autoradiograms, the guanines of the guanine-rich ODNs are numbered in alignment with ODN III as shown schematically above the autoradiograms. Protected guanines are indicated by closed ovals and unprotected guanines are indicated by open ovals, and the positions of the G → C substitutions in ODN VIII are indicated.

III, and myc1245. The footprints are characterized by the protection of four runs of three contiguous guanines and are consistent with the formation of a guanine quadruplex composed of three stracks of guanine tetrads. When the sequences are numbered from the 5′ end of ODN III (representing the beginning of the first run of guanines and corresponding to position −65 in the HIF-1α promoter), DMS protection is observed at G2-G4, G6-G8, G15-G17, and G19-G21. As one would expect, guanines 5′ and 3′ to the quadruplex forming region of the PPT, G1, G23, and G25 in ODN II, are reactive with DMS. In addition, four central guanines of ODN II and ODN III, G9, G11, G13, and G14, are also reactive with DMS. We interpret this pattern of DMS protection to be consistent with the formation of an intramolecular G-quadruplex composed of three stacked guanine tetrads in a configuration that places the central guanines in a loop composed of six nucleotides. ODN II and ODN III produced similar footprints, showing that the immediate flanking sequences are neither necessary nor detrimental to quadruplex formation. No protection from DMS methylation is seen for ODN I (the complementary sequence to ODN II). Similarly, ODN VIII (G → C substitution at the central guanine of each run of protected guanines) did not produce a DMS footprint, consistent with the lack of quadruplex formation when these runs of guanines are disrupted.

The folding of an ODN into an intramolecular quadruplex frequently makes the ODN more compact and migrate at a faster rate during gel electrophoresis, while the intermolecular association of multiple ODNs would be expected to result in complexes of slower mobility (*46*, *72*−*74*). In Figure 5A, we compare the electrophoretic mobility of the guanine-rich strand of the HIF-1α PPT with ODNs bearing mutations that disrupted G-quadruplex formation. The electrophoretic mobility of these ODNs was compared in a high-potassium gel, containing 140 mM KCl in the gel matrix to preserve the DNA secondary structures formed during incubation in 140 mM KCl prior to electrophoresis. ODN VIII (bearing four G → C substitutions) and ODN IX (bearing six mutations in the loop region) migrate as a single species in the gel, whether incubated in the presence or absence of 140 mM potassium before electrophoresis in the high-potassium gel. In contrast, ODN II forms multiple slower migrating species in the high-potassium gel that are consistent with the formation of bimolecular (2 stranded or 2s) and tetramolecular (4 stranded or 4s) G-quadruplexes. We demonstrated that the unimolecular G-quadruplex (1s) has the same electrophoretic mobility as the unstructured form of ODN

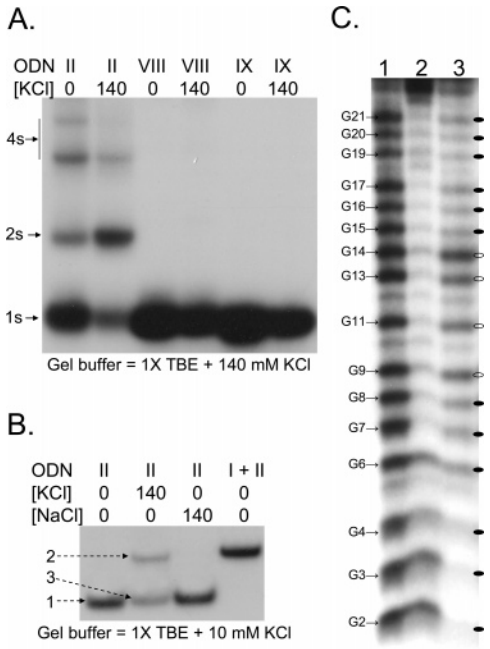

FIGURE 5: Electrophoretic mobility shift assays with the guanine-rich strand of the HIF-1α PPT. (A) ODN II migrates as unimolecular (1s), bimolecular (2s), and tetramolecular (4s) species in a high-potassium gel, while ODNs bearing substitution mutations in the runs of guanines (ODN VIII) or the loop region (ODN IX) migrate as a single, unimolecular species. (B) ODN II was incubated in 140 mM KCl, 140 mM NaCl, or no additional salt, and then DMS was added to each sample before loading onto a low-potassium (10 mM KCl) gel. Duplex DNA composed of ODN I + II was included for comparison as a size marker. After electrophoresis, the bands indicated by arrows were excised from the gel, and the ODNs were subjected to piperidine cleavage. (C) The piperidine cleavage reactions were resolved on a 10% sequencing gel. Protected guanines from the unimolecular species of ODN II with KCl from band 3 (in lane 3) are denoted by closed ovals while reactive guanines are denoted by open ovals, and this characteristic footprint demonstrates that the intramolecular G-quadruplex formed ODN II has the same electrophoretic migration as the unstructured form of the HIF-1α PPT.

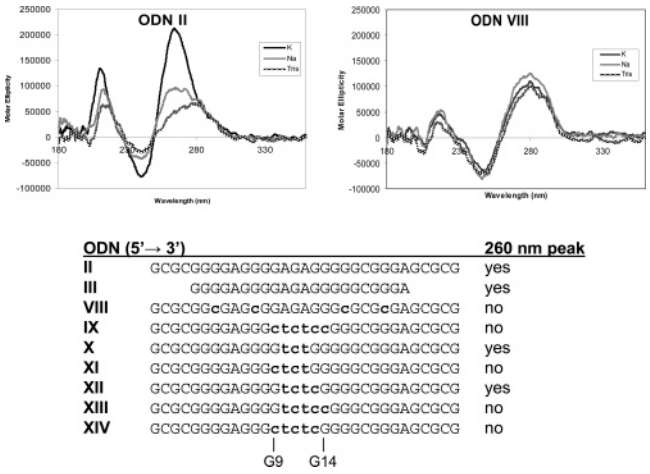

ODN (5'→ 3')		260 nm peak
II	GCGCGGGGAGGGGAGAGGGGGCGGGAGCGCG	yes
III	GGGGAGGGGAGAGGGGGCGGGA	yes
VIII	GCGCGGcGAGcGGAGAGGGcGCGcGAGCGCG	no
IX	GCGCGGGGAGGGctctccGGGCGGGAGCGCG	no
X	GCGCGGGGAGGGGtctGGGGGCGGGAGCGCG	yes
XI	GCGCGGGGAGGGctctGGGGGCGGGAGCGCG	no
XII	GCGCGGGGAGGGGtctcGGGGCGGGAGCGCG	yes
XIII	GCGCGGGGAGGGGtctccGGGCGGGAGCGCG	no
XIV	GCGCGGGGAGGGctctcGGGGCGGGAGCGCG	no

G9 G14

FIGURE 6: Circular dichroism spectroscopy with ODNs representing the PPT of the HIF-1α promoter. Spectra for ODN II, the native HIF-1α promoter sequence, and ODN VIII bearing mutations in the central guanines of each run are shown. Data for a series of ODNs lacking flanking sequence (ODN III) or bearing mutations in the loop region (ODNs IX−XIV) are summarized as either producing or lacking the characteristic potassium-dependent peak at 260 nm seen with ODN II. Loop mutants with disruption of G9 or G14 destabilize G-quadruplex formation.

II by treating the G-quadruplex reactions with DMS just prior to electrophoresis in a low-potassium gel (Figure 5B, containing 10 mM KCl in the gel matrix, a minimal concentration intended to preserve the most stable secondary structures formed before electrophoresis), followed by band excision, and piperidine cleavage to generate the DMS footprints shown in Figure 5C. In the absence of potassium before electrophoresis, ODN II migrates as a single species in the low-potassium gel (band 1) which does not produce a footprint. When ODN II is incubated with 140 mM potassium before electrophoresis, and bands comigrating with double-stranded ODN I + II (band 2) and single-stranded ODN II (band 3) are excised from the gel, DMS protection consistent with G-quadruplex formation is observed. The unimolecular G-quadruplex (band 3) comigrates with unstructured ODN II and produces a footprint identical to the footprints shown in Figure 4. The potassium-dependent slower mobility species in Figure 5B (band 2) is shown to be a bimolecular G-quadruplex, since it comigrates with duplex DNA (formed by annealing ODN II to its complement, ODN I) and produces an extended DMS footprint that includes the central guanines in the sequence. The slowest migrating potassium-dependent species formed by ODN II in Figure 5A (4s) are most likely tetramolecular G-quadruplexes, and they also produce an extended footprint that includes the central guanines (not shown). Interestingly, sodium ions do not appear to support stable G-quadruplex formation with this sequence under these conditions, since ODN II incubated in 140 mM sodium ions before electrophoresis migrates as a single species (Figure 5B) which does not produce a DMS footprint when excised from the gel (not shown).

G-quadruplexes have been probed by circular dichroism to deduce the orientation of the strands, because the parallel and antiparallel arrangement of the strands usually show characteristic spectra (*39*, *75*−*78*). The CD spectra of ODN II and VIII are compared in Figure 6. In potassium, ODN II produces a strong CD maximum at ∼260 nm, which is consistent with a parallel orientation of the strands in the G-quadruplex. In Tris buffer, the CD peak for ODN II widens and shifts to 280 nm, while in sodium, the CD spectrum appears to be intermediate between the spectrum for ODN II in potassium and ODN II in Tris buffer in the absence of a monovalent cation. ODN VIII, bearing a mutation in the central guanine of each run involved in G-quadruplex formation, produces a much different CD spectrum, with maxima at 280 nm in potassium, sodium, and Tris without monovalent cation. ODN III, lacking the flanking sequences outside the G-quadruplex forming region, yielded similar CD spectra to ODN II, with a positive peak at 260 nm, again consistent with the formation of a parallel G-quadruplex.

We evaluated a series of ODNs with alterations (G to C or A to T inversions) in the nucleotides (nt) of the predicted central loop of the G-quadruplex, summarized in Table 1. Collectively, these data demonstrated that alterations of G9, G14, or both tended to destabilize G-quadruplex formation. For example, ODN IX contains a 6 nt mutation of the entire loop region and does not produce the characteristic DMS footprint or CD spectrum of the HIF-1α G-quadruplex. ODN XI, XIII, and XIV, with 4−5 nt mutations starting at G9 or ending at G14, did not produce strong CD maxima at 260 nm and produced weak DMS footprints in potassium. ODN X and XII, with central 3−4 nt mutations produced strong

CD maxima at 260 nm and potassium-dependent DMS footprints similar to those shown for ODN II. These data demonstrate that the most central guanines in the loop, G11 and G13, do not participate in stabilizing the HIF-1α promoter G-quadruplex, but the two outer guanines in the loop, G9 and G14, may be needed for stable G-quadruplex formation. These observations are somewhat surprising in comparison to the myc1245 ODN, which has 6 nt substitutions in its central loop region, was shown elsewhere to form a stable G-quadruplex structure (*67*), and produced a strong DMS footprint in our studies. It is interesting to note that the guanine runs in myc1245 differ slightly from the runs of guanines in the HIF-1α ODNs by having runs of four guanines at both the 5′ and 3′ ends, while the HIF-1α ODNs lack the 3′ run of four guanines. Loop or flanking guanines may help to stabilize the G-quadruplex while not participating in the formation of the guanine tetrads.

We performed EMSA, DMS footprinting, and CD spectroscopy on several additional ODNs representing various segments of the HIF-1α PPT, summarized in Table 1. G-quadruplex forming sequences often occur within the context of a longer PPT. We wished to examine whether the polypurine sequences adjacent to the G-quadruplex forming sequence of the HIF-1α promoter were also capable of forming competing G-quadruplex structures using one or more additional runs of guanines. ODN V represents another PPT immediately downstream of the quadruplex forming sequence which also contains four runs of three or more contiguous guanines, albeit spaced at longer and less regular intervals. ODN V does not yield any structures of altered mobility on EMSA nor does it produce a DMS footprint. Extension of the quadruplex forming sequence to include a fifth run of guanines (ODN IV) resulted in increased number of altered mobility structures on EMSA and a shift to a broadened maxima positive peak from 260 to 280 nm, together suggesting the formation of a mixture of intermolecular and intramolecular structures with both parallel and antiparallel strand orientations. ODN VI represents an extended HIF-1α PPT (ODN II plus ODN V). ODNs IV and VI both form a core DMS footprint similar to the one seen with ODNs II and III in Figure 4. ODN VII represents a highly homologous sequence in the HIF-2α promoter and differs from the HIF-1α promoter (ODN II) by only 2 nt in the most upstream run of guanines in the quadruplex forming region. This small difference results in four runs of four contiguous guanines, and ODN VII produces a potassium-dependent DMS footprint consistent with the formation of four tetrad stacks as well a CD spectrum in potassium similar to that of ODN II. In summary, these data demonstrate that the sequence from −85 to −65 in the HIF-1α promoter is able to form a parallel, intramolecular G-quadruplex composed of three stacks of tetrads.

DNA polymerase arrest assays have been used as tools for the evaluation of DNA secondary structure formation based on the principle that the polymerase cannot efficiently traverse a stable DNA secondary structure, such as a G-quadruplex, and these assays have proven useful for screening for potential G-quadruplex interactive compounds capable of binding to a given sequence (*70*, *71*). In these assays, we annealed a primer (polP, Table 1) to a template containing either the HIF-1α quadruplex forming region (polH) or a random sequence control (polC), and then

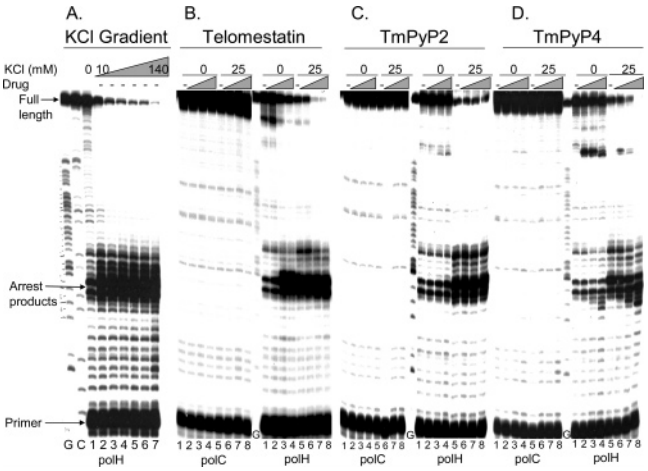

FIGURE 7: DNA polymerase arrest assays show that telomestatin and TmPyP4 can bind to and stabilize the G-quadruplex formed by the HIF-1α promoter. The primer, full-length primer extension products, and DNA polymerase arrest products are shown by arrows. The arrest products occur just before the first guanine of the G-quadruplex and are associated with a decrease in full-length primer extension. G and C ladders were obtained by chain termination sequencing. (A) Extension through the HIF-1α template (polH) after incubation in increasing concentrations of potassium (lane 1: 0 mM KCl; lane 2: 10 mM KCl; lane 3: 25 mM KCl; lane 4: 50 mM KCl; lane 5: 75 mM KCl; lane 6: 100 mM KCl; lane 7: 140 mM KCl). (B) The random sequence control (polC) and HIF-1α templates were treated with telomestatin. (C) Templates were treated with TmPyP2. (D) Templates were treated with TmPyP4. Each template was treated in the absence of drug (lanes 1 and 5), 0.1 μM drug (lanes 2 and 6), 0.5 μM drug (lanes 3 and 7), or 1 μM drug (lanes 4 and 8) in the absence (lanes 1−4) or presence of 25 mM KCl (lanes 5−8).

measured the ability of *taq* DNA polymerase to extend through the template sequence in the presence or absence of potassium and several G-quadruplex binding ligands (Figure 7). A DNA polymerase arrest assay was conducted on the PPT of the HIF-1α promoter (polH) over a concentration range of KCl (Figure 7A). This assay shows the potassium-dependent arrest of taq polymerase at the beginning of the PPT and shows that arrest products become prominent in potassium ion concentrations as low as 10 mM. There is a decrease in full-length primer extension as the potassium concentration is raised to intracellular levels (140 mM). At physiological potassium concentrations, polymerase arrest is almost complete, and we selected a lower potassium concentration, 25 mM, for the addition of potential G-quadruplex ligands so that a decrease in full-length extension products would be detectable and provide evidence of drug binding and stabilization of the G-quadruplex structure. For these assays, we also included a random sequence control template (polC) to rule out any effect of the compounds not due to interaction with the HIF-1α G-quadruplex. Telomestatin is a natural product that was shown to bind to the G-quadruplex formed by the telomeric repeat sequences (*63*, *79*−*82*). The addition of telomestatin (0.1−1.0 μM) to the random sequence control template had no effect on polymerase extension in the presence or absence of potassium ions (Figure 7B). In contrast, telomestatin induced DNA polymerase arrest at the HIF-1α G-quadruplex forming sequence in a dose-dependent manner even in the absence of potassium. In the presence of potassium, polymerase arrest was complete at 0.5−1.0 μM concentrations of telomestatin. These data demonstrate that telomestatin can both induce

and stabilize the HIF-1α G-quadruplex. TmPyP4 is a cationic porphyrin that has been shown to bind to the telomeric G-quadruplex and the human c-myc G-quadruplex, while TmPyP2 is a positional isomer of TmPyP4 that has a lower capacity for binding to G-quadruplexes (*58*, *63*, *65*, *83*). TmPyP2 (0.1−1.0 μM) had no effect on DNA polymerase arrest in the control template nor the HIF-1α template (Figure 7C). In contrast, TmPyP4 caused dose-dependent DNA polymerase arrest at the HIF-1α G-quadruplex forming region at concentrations of 0.5−1.0 μM in the presence of potassium ions but had no effect on the random sequence control template at any concentration tested (Figure 7D). These data demonstrate that TmPyP4 but not TmPyP2 is capable of binding to and stabilizing the G-quadruplex formed by the HIF-1α promoter.

DISCUSSION

In summary, we have demonstrated that a polypurine:polypyrimidine tract in the human HIF-1α promoter is needed for constitutive transcription of the HIF-1α gene. We have shown that the polypurine strand from this region from −65 to −85 (upstream of the transcription start site) can fold into an intramolecular G-quadruplex to produce a potassium-dependent DMS footprint and a characteristic circular dichroism spectrum indicative of a parallel arrangement of the four strands involved in tetraplex formation. We have shown that two G-quadruplex ligands, telomestatin and TmPyP4, are capable of binding to and stabilizing the G-quadruplex formed by the HIF-1α polypurine sequence. We have shown that specifically altering the sequence of the polypurine:polypyrimidine tract within the G-quadruplex forming region markedly reduces HIF-1α transcriptional activity, results that are in broad agreement with a previous HIF-1α promoter serial deletion analysis (*24*). It is interesting to note that the HIF-2α promoter contains a nearly identical polypurine/polypyrimidine tract, and while not the focus of these studies, the polypurine strand (ODN VII) also appears capable of forming an intramolecular G-quadruplex. These observations may indicate that there is a level of coordinate transcriptional regulation for the HIF-1α and HIF-2α genes based on a common structural motif in the promoter regions of these two hypoxia inducible genes that drive the cellular response to hypoxia.

The DMS footprint produced by the HIF-1α PPT suggests the formation of three stacked tetrads from a sequence with the general motif: $G_3N_1G_3N_6G_3N_1G_3$. A sequence derived from the c-myc oncogene, myc-1245, bears the same general sequence motif (Figure 4) and was structurally characterized by nuclear magnetic resonance (NMR) (*67*). These studies showed that when the myc sequence was modified by substitution of one run of guanines to reduce the number of competing structures, the resulting $G_3N_1G_3N_6G_3N_1G_3$ motif produced a parallel, propeller-type G-quadruplex composed of three stacks of G-tetrads and three double-chain-reversal loops. The central loop contained six nucleotides, while the other two loops contained only a single nucleotide. We believe that our data are consistent with a similar structure in the HIF-1α promoter. First, DMS footprints demonstrate that the two runs of three protected guanines at each end of the sequence are separated by guanines in the central loop region that are reactive with DMS. Second, the CD spectra of the HIF-1α G-quadruplex (ODNs II and III) have strong positive peaks at 260 nm, suggesting a parallel orientation of the runs of guanines involved in the formation of the G-tetrads. On the basis of these data, we infer that the HIF-1α promoter can form a parallel, propeller-type G-quadruplex. The presence of additional runs of guanines that could potentially participate in G-quadruplex formation is also similar to the G-quadruplex forming regions in the c-myc and muscle specific gene promoters. In the HIF-1α promoter, a fifth run of three guanines is present just downstream of the G-quadruplex forming region and could participate in the formation of alternate G-quadruplex structures. Indeed, although the region downstream of the −65 to −85 PPT contains multiple runs of guanines, this region (represented by ODN V) does not seem capable of forming a G-quadruplex by itself; however, extended PPTs encompassing −65 to −85 plus downstream sequences (ODN IV and VI) appear to form G-quadruplexes. It is possible that the downstream runs of guanines could form bimolecular G-quadruplexes with the upstream runs of guanines, and precedent for the formation of such complexes has recently been reported in several muscle specific gene promoters (*59*).

G-quaduplex structures in gene promoters could potentially repress or activate gene transcription. For example, a G-quadruplex structure in the human insulin-linked polymorphic region (ILPR) was suggested to enhance the transcription of this gene (*72*). Initial models of the G-quadruplex in the c-Myc promoter proposed an activating role for this structure in transcription (*55*). However, G-quadruplex formation stabilized by TmPyP4 repressed c-myc transcription, suggesting that the G-quadruplex is a transcriptional repressor (*57*). We suggest that the HIF-1α promoter represents another example of a gene that contains an important regulatory element capable of G-quadruplex formation. G-quadruplex formation in this region may be involved in positively or negatively regulating HIF-1α gene expression, and further studies will be needed to determine whether such structures play a role in HIF-1α transcription in the cell. It is important to note that the mutation we used to demonstrate the important role of the polypurine tract in HIF-1α transcription would be expected to abrogate the binding of two activating transcription factors, Sp1 and AP-2, from their putative binding sites, as well as prevent G-quadruplex formation. Further studies will be needed to determine the relative role of transcription factor binding and G-quadruplex formation in the polypurine tract on HIF-1α transcription. A DNA polymerase arrest assay demonstrated that two G-quadruplex ligands, telomestatin and TmPyP4 can bind to and stabilize the G-quadruplex formed by the HIF-1α promoter. Further studies will be needed to determine whether these molecules have an effect on HIF-1α gene expression. Small molecule inhibitors of HIF-1 are currently under investigation as anticancer therapeutics (*84*), and if G-quadruplex ligands were shown to repress HIF-1α expression, such agents could have applications to inhibit tumor angiogenesis and the ability of tumors to adapt to a hypoxic microenvironment.

SUPPORTING INFORMATION AVAILABLE

Extinction coefficients for oligonucleotides. This material is available free of charge via the Internet at http://pubs.acs.org.

REFERENCES

1. Safran, M., and Kaelin, W. G., Jr. (2003) HIF hydroxylation and the mammalian oxygen-sensing pathway, *J. Clin. Invest. 111*, 779−783.
2. Semenza, G. L. (2001) HIF-1 and mechanisms of hypoxia sensing, *Curr. Opin. Cell Biol. 13*, 167−171.
3. Zhong, H., De Marzo, A. M., Laughner, E., Lim, M., Hilton, D. A., Zagzag, D., Buechler, P., Isaacs, W. B., Semenza, G. L., and Simons, J. W. (1999) Overexpression of hypoxia-inducible factor 1alpha in common human cancers and their metastases, *Cancer Res. 59*, 5830−5835.
4. Semenza, G. L., Agani, F., Booth, G., Forsythe, J., Iyer, N., Jiang, B. H., Leung, S., Roe, R., Wiener, C., and Yu, A. (1997) Structural and functional analysis of hypoxia-inducible factor 1, *Kidney Int. 51*, 553−555.
5. Semenza, G. L. (2003) Targeting HIF-1 for cancer therapy, *Nat. Rev. Cancer 3*, 721−732.
6. Erler, J. T., Cawthorne, C. J., Williams, K. J., Koritzinsky, M., Wouters, B. G., Wilson, C., Miller, C., Demonacos, C., Stratford, I. J., and Dive, C. (2004) Hypoxia-mediated down-regulation of Bid and Bax in tumors occurs via hypoxia-inducible factor 1-dependent and -independent mechanisms and contributes to drug resistance, *Mol. Cell Biol. 24*, 2875−2889.
7. Ferrara, N. (2004) Vascular endothelial growth factor: basic science and clinical progress, *Endocr. Rev. 25*, 581−611.
8. Ebbinghaus, S. W., and Gordon, M. S. (2004) Renal cell carcinoma: rationale and development of therapeutic inhibitors of angiogenesis, *Hematol. Oncol. Clin. North Am. 18*, 1143−114x.
9. Zhou, J., Callapina, M., Goodall, G. J., and Brune, B. (2004) Functional integrity of nuclear factor kappaB, phosphatidylinositol 3′-kinase, and mitogen-activated protein kinase signaling allows tumor necrosis factor alpha-evoked Bcl-2 expression to provoke internal ribosome entry site-dependent translation of hypoxia-inducible factor 1alpha, *Cancer Res. 64*, 9041−9048.
10. Lang, K. J., Kappel, A., and Goodall, G. J. (2002) Hypoxia-inducible factor-1alpha mRNA contains an internal ribosome entry site that allows efficient translation during normoxia and hypoxia, *Mol. Biol. Cell 13*, 1792−1801.
11. Laughner, E., Taghavi, P., Chiles, K., Mahon, P. C., and Semenza, G. L. (2001) HER2 (neu) signaling increases the rate of hypoxia-inducible factor 1alpha (HIF-1alpha) synthesis: novel mechanism for HIF-1-mediated vascular endothelial growth factor expression, *Mol. Cell Biol. 21*, 3995−4004.
12. Page, E. L., Robitaille, G. A., Pouyssegur, J., and Richard, D. E. (2002) Induction of hypoxia-inducible factor-1alpha by transcriptional and translational mechanisms, *J. Biol. Chem. 277*, 48403−48409.
13. Treins, C., Giorgetti-Peraldi, S., Murdaca, J., Semenza, G. L., and Van, O. E. (2002) Insulin stimulates hypoxia-inducible factor 1 through a phosphatidylinositol 3-kinase/target of rapamycin-dependent signaling pathway, *J. Biol. Chem. 277*, 27975−27981.
14. Zhong, H., Chiles, K., Feldser, D., Laughner, E., Hanrahan, C., Georgescu, M. M., Simons, J. W., and Semenza, G. L. (2000) Modulation of hypoxia-inducible factor 1alpha expression by the epidermal growth factor/phosphatidylinositol 3-kinase/PTEN/AKT/FRAP pathway in human prostate cancer cells: implications for tumor angiogenesis and therapeutics, *Cancer Res. 60*, 1541−1545.
15. Dery, M. A., Michaud, M. D., and Richard, D. E. (2005) Hypoxia-inducible factor 1: regulation by hypoxic and non-hypoxic activators, *Int. J. Biochem. Cell Biol. 37*, 535−540.
16. Ladoux, A., and Frelin, C. (1997) Cardiac expressions of HIF-1 alpha and HLF/EPAS, two basic loop helix/PAS domain transcription factors involved in adaptative responses to hypoxic stresses, *Biochem. Biophys. Res. Commun. 240*, 552−556.
17. Wiener, C. M., Booth, G., and Semenza, G. L. (1996) In vivo expression of mRNAs encoding hypoxia-inducible factor 1, *Biochem. Biophys. Res. Commun. 225*, 485−488.
18. Palmer, L. A., Semenza, G. L., Stoler, M. H., and Johns, R. A. (1998) Hypoxia induces type II NOS gene expression in pulmonary artery endothelial cells via HIF-1, *Am. J. Physiol. 274*, L212-L219.
19. Wenger, R. H., Kvietikova, I., Rolfs, A., Gassmann, M., and Marti, H. H. (1997) Hypoxia-inducible factor-1 alpha is regulated at the post-mRNA level, *Kidney Int. 51*, 560−563.
20. Krieg, M., Haas, R., Brauch, H., Acker, T., Flamme, I., and Plate, K. H. (2000) Up-regulation of hypoxia-inducible factors HIF-1alpha and HIF-2alpha under normoxic conditions in renal carcinoma cells by von Hippel-Lindau tumor suppressor gene loss of function, *Oncogene 19*, 5435−5443.
21. Turner, K. J., Moore, J. W., Jones, A., Taylor, C. F., Cuthbert-Heavens, D., Han, C., Leek, R. D., Gatter, K. C., Maxwell, P. H., Ratcliffe, P. J., Cranston, D., and Harris, A. L. (2002) Expression of hypoxia-inducible factors in human renal cancer: relationship to angiogenesis and to the von Hippel-Lindau gene mutation, *Cancer Res. 62*, 2957−2961.
22. Blouin, C. C., Page, E. L., Soucy, G. M., and Richard, D. E. (2004) Hypoxic gene activation by lipopolysaccharide in macrophages: implication of hypoxia-inducible factor 1alpha, *Blood 103*, 1124−1130.
23. Iyer, N. V., Leung, S. W., and Semenza, G. L. (1998) The human hypoxia-inducible factor 1alpha gene: HIF1A structure and evolutionary conservation, *Genomics 52*, 159−165.
24. Minet, E., Ernest, I., Michel, G., Roland, I., Remacle, J., Raes, M., and Michiels, C. (1999) HIF1A gene transcription is dependent on a core promoter sequence encompassing activating and inhibiting sequences located upstream from the transcription initiation site and cis elements located within the 5′UTR, *Biochem. Biophys. Res. Commun. 261*, 534−540.
25. Hapgood, J. P., Riedemann, J., and Scherer, S. D. (2001) Regulation of gene expression by GC-rich DNA cis-elements, *Cell Biol. Int. 25*, 17−31.
26. Keniry, M. A. (2000) Quadruplex structures in nucleic acids, *Biopolymers 56*, 123−146.
27. Venczel, E. A., and Sen, D. (1996) Synapsable DNA, *J. Mol. Biol. 257*, 219−224.
28. Todd, A. K., Johnston, M., and Neidle, S. (2005) Highly prevalent putative quadruplex sequence motifs in human DNA, *Nucleic Acids Res. 33*, 2901−2907.
29. Huppert, J. L., and Balasubramanian, S. (2005) Prevalence of quadruplexes in the human genome, *Nucleic Acids Res. 33*, 2908−2916.
30. Schultze, P., Hud, N. V., Smith, F. W., and Feigon, J. (1999) The effect of sodium, potassium and ammonium ions on the conformation of the dimeric quadruplex formed by the Oxytricha nova telomere repeat oligonucleotide d(G(4)T(4)G(4)), *Nucleic Acids Res. 27*, 3018−3028.
31. Wang, Y., and Patel, D. J. (1992) Guanine residues in d(T2AG3) and d(T2G4) form parallel-stranded potassium cation stabilized G-quadruplexes with anti glycosidic torsion angles in solution, *Biochemistry 31*, 8112−8119.
32. Sen, D., and Gilbert, W. (1988) Formation of parallel four-stranded complexes by guanine-rich motifs in DNA and its implications for meiosis, *Nature 334*, 364−366.
33. Laughlan, G., Murchie, A. I., Norman, D. G., Moore, M. H., Moody, P. C., Lilley, D. M., and Luisi, B. (1994) The high-resolution crystal structure of a parallel-stranded guanine tetraplex, *Science 265*, 520−524.
34. Phillips, K., Dauter, Z., Murchie, A. I., Lilley, D. M., and Luisi, B. (1997) The crystal structure of a parallel-stranded guanine tetraplex at 0.95 Å resolution, *J. Mol. Biol. 273*, 171−182.
35. Sundquist, W. I., and Klug, A. (1989) Telomeric DNA dimerizes by formation of guanine tetrads between hairpin loops, *Nature 342*, 825−829.
36. Keniry, M. A., Strahan, G. D., Owen, E. A., and Shafer, R. H. (1995) Solution structure of the Na+ form of the dimeric guanine quadruplex [d(G3T4G3)]2, *Eur. J. Biochem. 233*, 631−643.
37. Sundquist, W. I., and Heaphy, S. (1993) Evidence for interstrand quadruplex formation in the dimerization of human immunodeficiency virus 1 genomic RNA, *Proc Natl. Acad. Sci. U.S.A. 90*, 3393−3397.
38. Dapic, V., Bates, P. J., Trent, J. O., Rodger, A., Thomas, S. D., and Miller, D. M. (2002) Antiproliferative activity of G-quartet-forming oligonucleotides with backbone and sugar modifications, *Biochemistry 41*, 3676−3685.
39. Dapic, V., Abdomerovic, V., Marrington, R., Peberdy, J., Rodger, A., Trent, J. O., and Bates, P. J. (2003) Biophysical and biological properties of quadruplex oligodeoxyribonucleotides, *Nucleic Acids Res. 31*, 2097−2107.
40. Henderson, E., Hardin, C. C., Walk, S. K., Tinoco, I., Jr., and Blackburn, E. H. (1987) Telomeric DNA oligonucleotides form novel intramolecular structures containing guanine-guanine base pairs, *Cell 51*, 899−908.
41. Henderson, E. R., Moore, M., and Malcolm, B. A. (1990) Telomere G-strand structure and function analyzed by chemical protection, base analogue substitution, and utilization by telomerase in vitro, *Biochemistry 29*, 732−737.

42. Macaya, R. F., Schultze, P., Smith, F. W., Roe, J. A., and Feigon, J. (1993) Thrombin-binding DNA aptamer forms a unimolecular quadruplex structure in solution, *Proc Natl. Acad. Sci. U.S.A. 90*, 3745−3749.
43. Parkinson, G. N., Lee, M. P., and Neidle, S. (2002) Crystal structure of parallel quadruplexes from human telomeric DNA, *Nature 417*, 876−880.
44. Wang, Y., and Patel, D. J. (1993) Solution structure of the human telomeric repeat d[AG3(T2AG3)3] G-tetraplex, *Structure. 1*, 263−282.
45. Wang, Y., and Patel, D. J. (1995) Solution structure of the Oxytricha telomeric repeat d[G4(T4G4)3] G-tetraplex, *J. Mol. Biol. 251*, 76−94.
46. He, Y., Neumann, R. D., and Panyutin, I. G. (2004) Intramolecular quadruplex conformation of human telomeric DNA assessed with 125I-radioprobing, *Nucleic Acids Res. 32*, 5359−5367.
47. Williamson, J. R., Raghuraman, M. K., and Cech, T. R. (1989) Monovalent cation-induced structure of telomeric DNA: the G-quartet model, *Cell 59*, 871−880.
48. Guschlbauer, W., Chantot, J. F., and Thiele, D. (1990) Four-stranded nucleic acid structures 25 years later: from guanosine gels to telomer DNA, *J. Biomol. Struct. Dyn. 8*, 491−511.
49. Schaffitzel, C., Berger, I., Postberg, J., Hanes, J., Lipps, H. J., and Pluckthun, A. (2001) In vitro generated antibodies specific for telomeric guanine-quadruplex DNA react with Stylonychia lemnae macronuclei, *Proc Natl. Acad. Sci. U.S.A. 98*, 8572−8577.
50. Sen, D., and Gilbert, W. (1990) A sodium−potassium switch in the formation of four-stranded G4-DNA, *Nature 344*, 410−414.
51. Catasti, P., Chen, X., Moyzis, R. K., Bradbury, E. M., and Gupta, G. (1996) Structure−function correlations of the insulin-linked polymorphic region, *J. Mol. Biol. 264*, 534−545.
52. Fry, M., and Loeb, L. A. (1994) The fragile X syndrome d(CGG)n nucleotide repeats form a stable tetrahelical structure, *Proc Natl. Acad. Sci. U.S.A. 91*, 4950−4954.
53. Usdin, K., and Woodford, K. J. (1995) CGG repeats associated with DNA instability and chromosome fragility form structures that block DNA synthesis in vitro, *Nucleic Acids Res. 23*, 4202−4209.
54. Arthanari, H., and Bolton, P. H. (2001) Functional and dysfunctional roles of quadruplex DNA in cells, *Chem. Biol. 8*, 221−230.
55. Simonsson, T., Pecinka, P., and Kubista, M. (1998) DNA tetraplex formation in the control region of c-myc, *Nucleic Acids Res. 26*, 1167−1172.
56. Simonsson, T., and Henriksson, M. (2002) c-myc Suppression in Burkitt's lymphoma cells, *Biochem. Biophys. Res. Commun. 290*, 11−15.
57. Siddiqui-Jain, A., Grand, C. L., Bearss, D. J., and Hurley, L. H. (2002) Direct evidence for a G-quadruplex in a promoter region and its targeting with a small molecule to repress c-MYC transcription, *Proc Natl. Acad. Sci. U.S.A. 99*, 11593−11598.
58. Grand, C. L., Han, H., Munoz, R. M., Weitman, S., Von Hoff, D. D., Hurley, L. H., and Bearss, D. J. (2002) The cationic porphyrin TMPyP4 down-regulates c-MYC and human telomerase reverse transcriptase expression and inhibits tumor growth in vivo, *Mol. Cancer Ther. 1*, 565−573.
59. Yafe, A., Etzioni, S., Weisman-Shomer, P., and Fry, M. (2005) Formation and properties of hairpin and tetraplex structures of guanine-rich regulatory sequences of muscle-specific genes, *Nucleic Acids Res. 33*, 2887−2900.
60. Burger, A. M., Dai, F., Schultes, C. M., Reszka, A. P., Moore, M. J., Double, J. A., and Neidle, S. (2005) The G-quadruplex-interactive molecule BRACO-19 inhibits tumor growth, consistent with telomere targeting and interference with telomerase function, *Cancer Res. 65*, 1489−1496.
61. Rezler, E. M., Bearss, D. J., and Hurley, L. H. (2003) Telomere inhibition and telomere disruption as processes for drug targeting, *Annu. Rev. Pharmacol. Toxicol. 43*, 359−379.
62. Pennarun, G., Granotier, C., Gauthier, L. R., Gomez, D., Hoffschir, F., Mandine, E., Riou, J. F., Mergny, J. L., Mailliet, P., and Boussin, F. D. (2005) Apoptosis related to telomere instability and cell cycle alterations in human glioma cells treated by new highly selective G-quadruplex ligands, *Oncogene 24*, 2917−2928.
63. Kim, M. Y., Gleason-Guzman, M., Izbicka, E., Nishioka, D., and Hurley, L. H. (2003) The different biological effects of telomestatin and TMPyP4 can be attributed to their selectivity for interaction with intramolecular or intermolecular G-quadruplex structures, *Cancer Res. 63*, 3247−3256.
64. Lemarteleur, T., Gomez, D., Paterski, R., Mandine, E., Mailliet, P., and Riou, J. F. (2004) Stabilization of the c-myc gene promoter quadruplex by specific ligands' inhibitors of telomerase, *Biochem. Biophys. Res. Commun. 323*, 802−808.
65. Seenisamy, J., Rezler, E. M., Powell, T. J., Tye, D., Gokhale, V., Joshi, C. S., Siddiqui-Jain, A., and Hurley, L. H. (2004) The dynamic character of the G-quadruplex element in the c-MYC promoter and modification by TMPyP4, *J. Am. Chem. Soc. 126*, 8702−8709.
66. Maiti, S., Chaudhury, N. K., and Chowdhury, S. (2003) Hoechst 33258 binds to G-quadruplex in the promoter region of human c-myc, *Biochem. Biophys. Res. Commun. 310*, 505−512.
67. Phan, A. T., Modi, Y. S., and Patel, D. J. (2004) Propeller-type parallel-stranded G-quadruplexes in the human c-myc promoter, *J. Am. Chem. Soc. 126*, 8710−8716.
68. Ambrus, A., Chen, D., Dai, J., Jones, R. A., and Yang, D. (2005) Solution structure of the biologically relevant G-quadruplex element in the human c-MYC promoter. Implications for G-quadruplex stabilization, *Biochemistry 44*, 2048−2058.
69. Sambrook, J., and Russell, D. W. (2001) *Molecular Cloning, A Laboratory Manual*, Cold Spring Harbor Laboratory Press, Cold Spring Harbor, NY.
70. Weitzmann, M. N., Woodford, K. J., and Usdin, K. (1996) The development and use of a DNA polymerase arrest assay for the evaluation of parameters affecting intrastrand tetraplex formation, *J. Biol. Chem. 271*, 20958−20964.
71. Han, H., Hurley, L. H., and Salazar, M. (1999) A DNA polymerase stop assay for G-quadruplex-interactive compounds, *Nucleic Acids Res. 27*, 537−542.
72. Lew, A., Rutter, W. J., and Kennedy, G. C. (2000) Unusual DNA structure of the diabetes susceptibility locus IDDM2 and its effect on transcription by the insulin promoter factor Pur-1/MAZ, *Proc Natl. Acad. Sci. U.S.A. 97*, 12508−12512.
73. Han, H., Cliff, C. L., and Hurley, L. H. (1999) Accelerated assembly of G-quadruplex structures by a small molecule, *Biochemistry 38*, 6981−6986.
74. Han, H., Langley, D. R., Rangan, A., and Hurley, L. H. (2001) Selective interactions of cationic porphyrins with G-quadruplex structures, *J. Am. Chem. Soc. 123*, 8902−8913.
75. Lu, M., Guo, Q., and Kallenbach, N. R. (1992) Structure and stability of sodium and potassium complexes of dT4G4 and dT4G4T, *Biochemistry 31*, 2455−2459.
76. Balagurumoorthy, P., Brahmachari, S. K., Mohanty, D., Bansal, M., and Sasisekharan, V. (1992) Hairpin and parallel quartet structures for telomeric sequences, *Nucleic Acids Res. 20*, 4061−4067.
77. Balagurumoorthy, P. and Brahmachari, S. K. (1994) Structure and stability of human telomeric sequence, *J. Biol. Chem. 269*, 21858−21869.
78. Ren, J., Qu, X., Trent, J. O., and Chaires, J. B. (2002) Tiny telomere DNA, *Nucleic Acids Res. 30*, 2307−2315.
79. Kim, M. Y., Vankayalapati, H., Shin-Ya, K., Wierzba, K., and Hurley, L. H. (2002) Telomestatin, a potent telomerase inhibitor that interacts quite specifically with the human telomeric intramolecular g-quadruplex, *J. Am Chem. Soc 124*, 2098−2099.
80. Rosu, F., Gabelica, V., Shin-Ya, K., and De Pauw, E. (2003) Telomestatin-induced stabilization of the human telomeric DNA quadruplex monitored by electrospray mass spectrometry, *Chem. Commun. (Cambr.)* 2702−2703.
81. Gomez, D., Paterski, R., Lemarteleur, T., Shin-Ya, K., Mergny, J. L., and Riou, J. F. (2004) Interaction of telomestatin with the telomeric single-strand overhang, *J. Biol. Chem. 279*, 41487−41494.
82. Rezler, E. M., Seenisamy, J., Bashyam, S., Kim, M. Y., White, E., Wilson, W. D., and Hurley, L. H. (2005) Telomestatin and Diseleno Sapphyrin Bind Selectively to Two Different Forms of the Human Telomeric G-Quadruplex Structure, *J. Am Chem. Soc. 127*, 9439−9447.
83. Weisman-Shomer, P., Cohen, E., Hershco, I., Khateb, S., Wolfovitz-Barchad, O., Hurley, L. H., and Fry, M. (2003) The cationic porphyrin TMPyP4 destabilizes the tetraplex form of the fragile X syndrome expanded sequence d(CGG)n, *Nucleic Acids Res. 31*, 3963−3970.
84. Powis, G., and Kirkpatrick, L. (2004) Hypoxia inducible factor-1alpha as a cancer drug target, *Mol. Cancer Ther. 3*, 647−654.

BI051618U